

Ultrasonic measurements of the mechanical relaxations and complex stiffnesses in oriented linear polyethylene

W. P. Leung, F. C. Chen and C. L. Choy

Department of Physics, The Chinese University of Hong Kong, Hong Kong

and A. Richardson and I. M. Ward

Department of Physics, University of Leeds, Leeds LS2 9JT, UK

(Received 7 March 1983)

The five complex stiffnesses of highly oriented linear polyethylene produced by hydrostatic extrusion and die drawing have been determined by ultrasonic measurements. The results are compared with the elastic stiffnesses for crystalline polyethylene calculated theoretically. The development of anisotropic mechanical behaviour with draw ratio is discussed in terms of present structural understanding of highly oriented polyethylene. Although the very high stiffnesses obtained at the highest draw ratios are attributed to increasing crystal continuity, it is noted that the development of anisotropy in terms of low-temperature ultrasonic behaviour can be predicted to a good approximation by the reorienting unit aggregate model. This surprising result suggests that the overall orientation may still be the key parameter at low temperatures and high frequencies where there is no molecular mobility in the structure.

Keywords Ultrasonic measurements; complex stiffness; oriented polyethylene

INTRODUCTION

In recent years there have been several publications describing the dynamic mechanical behaviour of ultra-oriented linear polyethylene (LPE)¹⁻⁴. The measurements have mostly been undertaken at low frequencies (1–10 Hz) and confined to extensional, bending or shear modes of deformation. Some measurements have been made at ultrasonic frequencies⁵, the complex stiffnesses being determined at room temperature for oriented samples prepared by tensile drawing.

There is particular interest in determining all five independent stiffnesses for highly oriented uniaxial LPE. First, comparison can then be made with theoretical estimates for the elastic anisotropy. Secondly, the results can be examined in the light of structural models for the development of mechanical anisotropy in oriented polymers. Finally, it is valuable to examine the changes in the mechanical relaxation behaviour associated with the structural changes caused by the very high degrees of plastic deformation.

The present paper describes 10 MHz ultrasonic measurements of all five complex stiffnesses of transversely isotropic LPE samples produced by hydrostatic extrusion and die drawing. A detailed comparison is presented of the results with previous data, and with theoretical expectations. The experimental approach and some aspects of the interpretation follow that of a previous recent publication⁶.

EXPERIMENTAL

Preparation of samples

Hydrostatic extrusion. Oriented rods of LPE were

prepared by hydrostatic extrusion at 100°C of solid cylindrical billets through a conical die to a final bore diameter of 1.9–2.5 cm. Further details of the hydrostatic extrusion process are given in previous publications^{3,7}. Two grades of LPE were used, Rigidex 50 ($M_w = 101\,450$, $M_n = 6180$) where deformation ratios of 5 and 10 were obtained and Rigidex 40 ($M_w = 93\,600$, $M_n = 9600$) where a deformation ratio of 15 was obtained.

Die drawing. In the highest deformation ratios of 15 and 20, oriented samples of Rigidex 50 were also prepared by die drawing. In this technique a solid cylindrical billet is pulled through a heated conical die. In general, the material will leave the die wall at some point within the conical region, and tensile drawing continues until it is gradually frozen out at some distance from the die. Full details of the process, including results for LPE are given in previous publications^{8,9}.

Ultrasonic measurements

The ultrasonic measurements have been described in detail previously^{6,10} and will not be repeated here. In the range of 0° to 50°C, the water-tank method⁶ was employed to determine all five independent stiffnesses, C_{11} , C_{12} , C_{13} , C_{33} and C_{44} . The estimated errors of these measurements are about 2% for the directly measured C_{11} and C_{66} ($=\frac{1}{2}(C_{11} - C_{12})$) and 4–7% for the other moduli.

The stiffnesses C_{11} and C_{33} , as well as the corresponding loss tangents $\tan \delta_{11}$ and $\tan \delta_{33}$ were also measured from –120° to 100°C using the method of direct contact¹⁰. Propanol was used as the bonding medium from –120°C to room temperature, and silicone fluid (Edwards 704) was used at higher temperature. The accuracy of the storage stiffness and loss tangent is estimated to be 2% and 10%, respectively.

Table 1 Elastic constants for highly oriented LPE (draw ratio 20) at 0°C obtained from ultrasonic measurements

$C_{ij} =$	6.9	3.9	4.4	0	0	0	GPa
	3.9	6.9	4.4	0	0	0	
	4.4	4.4	66	0	0	0	
	0	0	0	1.6	0	0	
	0	0	0	0	1.6	0	
	0	0	0	0	0	1.5	
$S_{ij} =$	21	-11	-0.7	0	0	0	(GPa) ⁻¹ x 100
	-11	21	-0.7	0	0	0	
	-0.7	-0.7	1.6	0	0	0	
	0	0	0	64	0	0	
	0	0	0	0	64	0	
	0	0	0	0	0	66	

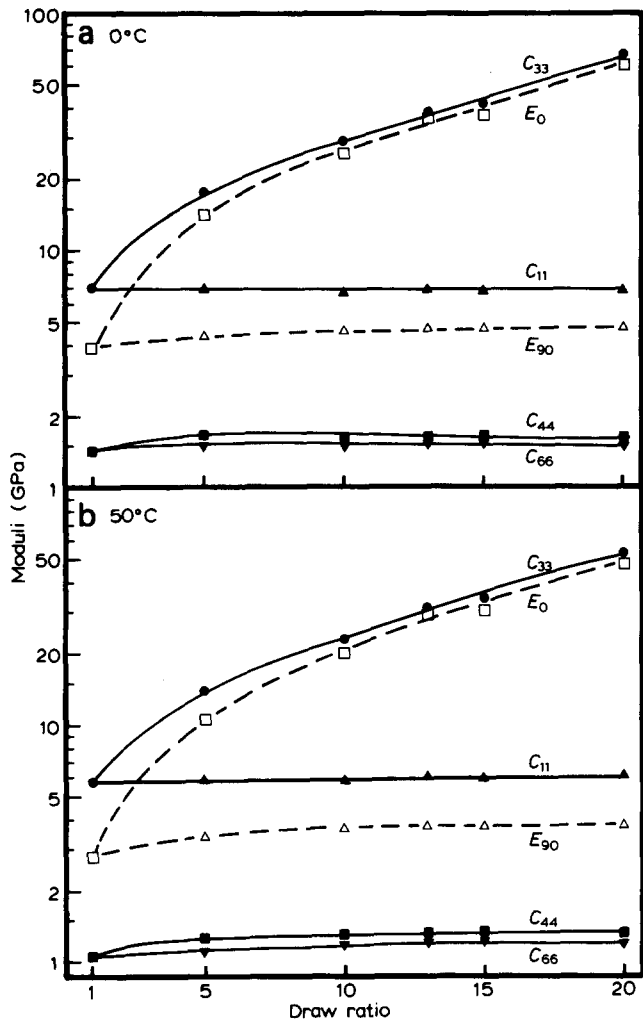


Figure 1 Draw ratio dependence of the elastic moduli of LPE at (a) 0°C and (b) 50°C

RESULTS AND DISCUSSION

The ultrasonic results for the most highly oriented sample ($\lambda = 20$) obtained at 0°C are summarized in the stiffness and compliance matrices shown in Table 1. The draw ratio dependence of the extensional and shear stiffnesses at 0° and 50°C is shown in Figure 1, and the temperature dependence of C_{11} , C_{33} , $\tan \delta_{11}$ and $\tan \delta_{33}$ in Figure 2.

Comparison of ultrasonic and low-frequency measurements

It is interesting to compare the ultrasonic results with previous data for highly oriented LPE, where different measurement techniques were used^{2,4,11,12}.

Table 2 provides a summary of the previous data, and in spite of very great differences in the frequency of measurement, comparison with the present results shows no significant discrepancies. The stiffness constant C_{33} or $E_0 (= 1/S_{33})$ is most sensitive to the degree of orientation, and also to temperature. The value of about 120 GPa obtained at -120°C from the present measurements for the $\lambda = 20$ sample is very consistent with previous dynamical mechanical measurements in tension² at 20 Hz where 160 GPa was obtained for $\lambda = 30$ at -175°C and in bending³ at 3.6 Hz where 105 GPa was obtained for $\lambda = 20$ at -175°C.

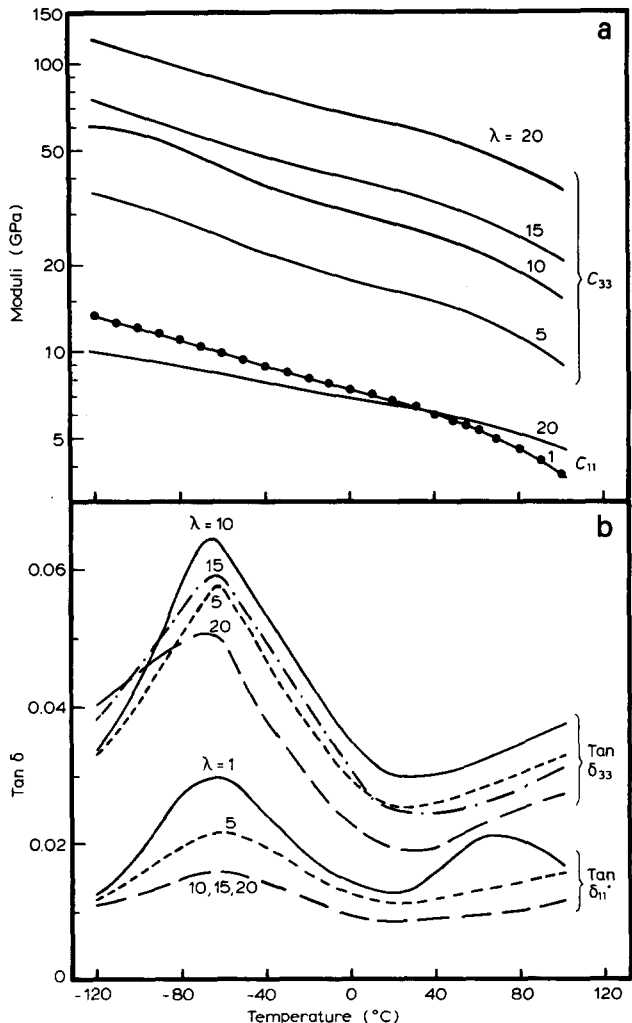


Figure 2 Temperature dependence of (a) the axial and transverse extensional moduli, C_{33} and C_{11} , and (b) the corresponding loss factors, $\tan \delta_{33}$ and $\tan \delta_{11}$ for LPE

Table 2 Comparison of measured mechanical stiffness with theoretical predictions

	Measured value		Theory ^{14,15}
	-175°C	20°C	
Axial Young's modulus ² (GPa); $\lambda = 30-35$ (20 Hz)	160	100	260-320
Transverse Young's modulus ¹¹ (GPa); $\lambda = 25$, 1-2 min loading	—	1.35	5-10
Shear modulus ⁴ (GPa); $\lambda = 25$ (1 Hz)	1.9	1.3	1-3
Poisson's ratio ^{12,13} ; $\lambda = 20-24$, 1 min loading	—	0.4-0.6	0.01-0.6

C_{11} and E_{90} ($=1/S_{11}$) are comparatively insensitive to draw ratio, but also show very significant temperature and frequency dependence. At $\lambda=20$, the ultrasonic measurements show a rise in C_{11} from 4.6 GPa at 100°C to 10.0 GPa at -120°C. A value for E_{90} of 1.35 GPa was obtained from Hertz compression measurements at 0°C (1-2 min loading) for a $\lambda=25$ sample. This compares with $E_{90}=4.7$ GPa at 0°C for a $\lambda=20$ sample measured ultrasonically.

The shear compliance and stiffness constants were only measured in the temperature range 0°-50°C where comparatively small temperature dependence is shown. The ultrasonic value for C_{44} of 1.57 GPa at 0°C for a sample with $\lambda=20$ can be compared with values of 1.4 GPa and 1.95 GPa at -55° and -196°C obtained from torsion pendulum measurements at 1 Hz on a sample with $\lambda=25$. The two types of measurement are in good agreement and show that at high frequencies and low temperatures a value of ~2 GPa is to be expected for C_{44} .

Finally, it is interesting to note that the ultrasonic data give values for the Poisson's ratios

$$\nu_{12} = -\frac{S_{12}}{S_{11}} \quad \text{and} \quad \nu_{13} = -\frac{S_{13}}{S_{33}}$$

in the range 0.4-0.6 which are consistent with the values of

$$\nu_{23} = -\frac{S_{23}}{S_{33}}$$

obtained by Michelson interferometry¹² and the Hall effect technique¹³ for highly oriented LPE sheets which possess orthorhombic symmetry, in distinction to the transverse isotropy of the oriented LPE rods.

Comparison with theoretical predictions

The elastic stiffness in the chain axis direction can be estimated using force constants from spectroscopic data. Most simply, only two modes of deformation, bond stretching and bond angle opening, need be considered, but more sophisticated calculations also include internal rotation around bonds in the chain. The other elastic constants include intermolecular forces between chains, and have been obtained using the lattice dynamical theory of Born and Huang¹⁶. The earliest complete set of elastic constants for polyethylene was given by Odajima and Maeda¹⁴. The precise values obtained depend on

estimates of the intermolecular force constants obtained from consideration of the lattice energy and on the unit cell dimensions, being especially sensitive to the setting angle, which defines the angle made by the planar zig-zag chain with the *b*-axis. Table 3 shows the stiffness and compliance matrices predicted by Odajima and Maeda¹⁴ on the basis of two independent sets of intermolecular potential functions, together with a more recent calculation by Tashiro *et al.*¹⁵

The comparison of the results shown in Tables 1 and 3 is very interesting. The measured stiffness C_{33} at 0°C is 66 GPa, which is about half the value at -120°C but is already approaching the theoretical value. The general pattern of anisotropy observed is also very much in line with theoretical predictions. The value for S_{11} of 21×10^{-2} (GPa)⁻¹ is within the predicted range $(14.5-21.1) \times 10^{-2}$ (GPa)⁻¹. The measured shear compliances of $S_{44}=63.7 \times 10^{-2}$ (GPa)⁻¹ and $S_{66}=65.8 \times 10^{-2}$ (GPa)⁻¹ are also quite close to the predicted values. The situation with regard to the lateral compliance constants S_{12} and S_{13} is less clear-cut, because there is a very wide difference between individual theoretical estimates. In the case of S_{12} , the calculations by Tashiro *et al.* suggest a Poisson's ratio $\nu_{12} \sim 0.5$ which is close to that observed, but the predicted Poisson's ratio ν_{13} is close to zero which is very much at variance with the experimental data. This particular result is clearly very sensitive to the details of the theoretical calculations.

Temperature and frequency dependence

The results for C_{33} and C_{11} shown in Figure 2 confirm previous dynamic mechanical measurements at low frequencies, indicating a strong temperature dependence of behaviour. Figure 3 shows the temperature of the γ -relaxation peak on a log frequency vs. reciprocal temperature plot together with data from dynamic mechanical and dielectric relaxation measurements^{3,4,17,19}. An activation energy of 14.2 kcal mol⁻¹ is obtained, which is in good agreement with previous work. The α -relaxation peak is not identifiable in the ultrasonic measurements and it can be concluded that at such high frequencies its position moves to temperatures above 100°C.

There is a substantial reduction in the magnitude of the γ -relaxation peak in $\tan \delta_{11}$ with increasing draw ratio. This is consistent with the view that this relaxation is primarily associated with the amorphous regions where mobility is reduced with increasing draw ratio. The comparative insensitivity of $\tan \delta_{33}$ to draw ratio observed here is at variance with low-frequency dynamical mechanical data where a significant reduction in relaxation strength was observed.

Structural interpretation of mechanical anisotropy

In general terms there are three aspects to structural understanding of the anisotropic mechanical behaviour.

First, at low temperatures the behaviour of the most highly oriented sample is approaching the theoretical behaviour predicted for fully oriented LPE. The influence of draw ratio is most evident for C_{33} and it has been suggested that this relates to the increase in the intercrystalline bridge content with increasing draw ratio³. At temperatures below the γ -relaxation there is also a small but significant contribution to the stiffness from the oriented non-crystalline regions⁴.

There are much smaller changes in the other elastic

Table 3 Elastic constants for polyethylene crystal

(a) Odajima and Maeda¹⁴

$$C_{ij} = \begin{pmatrix} 4.83 & 1.16 & 2.55 & 0 & 0 & 0 \\ 1.16 & 8.71 & 5.84 & 0 & 0 & 0 \\ 2.55 & 5.84 & 257.1 & 0 & 0 & 0 \\ 0 & 0 & 0 & 2.83 & 0 & 0 \\ 0 & 0 & 0 & 0 & 0.78 & 0 \\ 0 & 0 & 0 & 0 & 0 & 2.06 \end{pmatrix} \text{ GPa}$$

$$S_{ij} = \begin{pmatrix} 21.1 & -2.76 & -0.15 & 0 & 0 & 0 \\ -2.76 & 12.0 & -0.25 & 0 & 0 & 0 \\ -0.15 & -0.25 & 0.396 & 0 & 0 & 0 \\ 0 & 0 & 0 & 35.3 & 0 & 0 \\ 0 & 0 & 0 & 0 & 12.8 & 0 \\ 0 & 0 & 0 & 0 & 0 & 48.5 \end{pmatrix} (\text{GPa})^{-1} \times 100$$

(b) Odajima and Maeda¹⁴

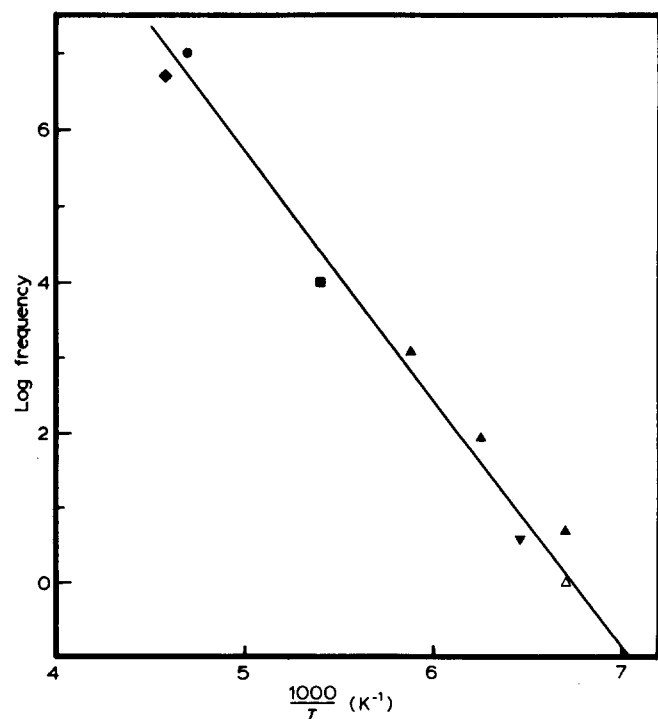
$$C_{ij} = \begin{pmatrix} 6.28 & 2.18 & 2.90 & 0 & 0 & 0 \\ 2.18 & 9.35 & 6.07 & 0 & 0 & 0 \\ 2.90 & 6.07 & 257.2 & 0 & 0 & 0 \\ 0 & 0 & 0 & 2.93 & 0 & 0 \\ 0 & 0 & 0 & 0 & 0.88 & 0 \\ 0 & 0 & 0 & 0 & 0 & 2.97 \end{pmatrix} \text{ GPa}$$

$$S_{ij} = \begin{pmatrix} 17.4 & -3.98 & -0.10 & 0 & 0 & 0 \\ -3.98 & 11.8 & -0.23 & 0 & 0 & 0 \\ -0.15 & -0.23 & 0.395 & 0 & 0 & 0 \\ 0 & 0 & 0 & 34.1 & 0 & 0 \\ 0 & 0 & 0 & 0 & 11.4 & 0 \\ 0 & 0 & 0 & 0 & 0 & 33.7 \end{pmatrix} (\text{GPa})^{-1} \times 100$$

(c) Tashiro et al.¹⁵

$$C_{ij} = \begin{pmatrix} 7.99 & 3.28 & 1.13 & 0 & 0 & 0 \\ 3.28 & 9.92 & 2.14 & 0 & 0 & 0 \\ 1.13 & 2.14 & 315.9 & 0 & 0 & 0 \\ 0 & 0 & 0 & 3.19 & 0 & 0 \\ 0 & 0 & 0 & 0 & 1.62 & 0 \\ 0 & 0 & 0 & 0 & 0 & 3.62 \end{pmatrix} \text{ GPa}$$

$$S_{ij} = \begin{pmatrix} 14.5 & -4.78 & -0.02 & 0 & 0 & 0 \\ -4.78 & 11.67 & -0.06 & 0 & 0 & 0 \\ -0.02 & -0.06 & 0.32 & 0 & 0 & 0 \\ 0 & 0 & 0 & 31.3 & 0 & 0 \\ 0 & 0 & 0 & 0 & 61.8 & 0 \\ 0 & 0 & 0 & 0 & 0 & 27.6 \end{pmatrix} (\text{GPa})^{-1} \times 100$$



stiffnesses with draw ratio, but it is notable that C_{11} shows a crossover in behaviour with increasing temperature (see Figure 2). This result is exactly similar to that observed in the dynamic mechanical results for the longitudinal shear stiffness C_{44} . In general terms it is considered that the crossovers in transverse stiffness C_{11} and shear stiffness C_{44} arise for the same reason⁴. At high temperatures where the non-crystalline material is very compliant, the behaviour is dominated by the stiffening effects of the intercrystalline bridges. At low temperatures on the other hand, the non-crystalline regions are rigid and the behaviour can be modelled to a first approximation by the single phase aggregate model²⁰. At high temperature all the elastic stiffnesses are increased by the stiffening effects of the intercrystalline bridges. At low temperatures, the behaviour relates to a first approximation to the overall molecular orientation only. Hence C_{33} increases and C_{11} decreases with increasing draw ratio over the value for the unoriented polymer.

Figure 3 Plot of log frequency versus $1/T$ for LPE: Δ , torsional ($\lambda=1-25$); \blacktriangle , tensile ($\lambda=1-25$); \triangle , flexural ($\lambda=12$); \blacksquare , dielectric ($\lambda=1$ and 4); \blacklozenge , longitudinal wave ($\lambda=12$); \bullet , present results ($\lambda=1-20$). All the mechanical data are obtained from plots of $\tan \delta$ vs. temperature, while the dielectric data are obtained from plots of ϵ'' vs. temperature

Secondly, as in previous publications, there is the question of the possible applicability of the aggregate model. This can be tested in two ways. First, the Reuss (uniform stress) and Voigt (uniform strain) bounds for the Young's modulus and shear modulus of the isotropic polymer can be calculated on the basis that this is an aggregate of units with the elastic constants determined at each draw ratio. The comparison of these values with the experimental values is shown in Table 4. Secondly, the actual pattern of mechanical anisotropy can be predicted on the reorienting unit aggregate model. This requires additional information or assumptions. In the first instance the elastic constants of a fully oriented sample are required. In this case, following the precedent of previous publications, this is based on the behaviour of the sample for $\lambda=20$. Furthermore, the orientation functions are required as a function of draw ratio. As a first approximation the pseudo-affine deformation scheme has been adopted. The results of these calculations are shown in Figure 4.

In spite of the dramatic changes in morphology which occur on drawing, it appears that the experimental data are quite close to the predicted Reuss (lower) bound. This rather surprising result is similar to that obtained previously for polypropylene^{6,21}, and suggests that the single phase aggregate model may still be applicable provided that the experimental frequency and temperature are such that the non-crystalline regions are essentially rigid.

Finally, there is the behaviour of the α - and γ -relaxation processes. In this case the ultrasonic measurements do not provide any new information. Previous dynamic mechanical measurements showed a reduction in the magnitude of the γ -relaxation with increasing draw ratio, which is consistent with modelling the behaviour in terms of a short fibre composite⁴. Although $\tan \delta_{11}$ shows a decrease in magnitude with increasing draw ratio, the results for $\tan \delta_{33}$ are not very convincing in this respect. It is considered that it is more difficult to interpret the magnitude of the ultrasonic $\tan \delta$ because the ultrasonic loss factor is associated with the scattering of sound waves, and would therefore be expected to be sensitive to structural features such as voids and crystalline-amorphous interfaces in the polymer. The high background value for $\tan \delta$ in the ultrasonic measurements as compared to that in low-frequency dynamic mechanical measurements is probably a reflection of the complex scattering processes.

The isotropic sample shows a peak at about 70°C which disappears on drawing (Figure 2). This peak was previously assigned by Waterman¹⁹ to the β -relaxation; as mentioned above the α -relaxation will be located above 100°C.

Table 4 Calculated values of isotropic elastic constants at 0°C

	Draw ratio					
	1	5	10	13	15	20
E^{iso} (Reuss)	4.00	4.91	4.91	5.05	5.20	5.00
G^{iso} (Reuss)	1.46	1.82	1.83	1.89	1.93	1.86
E^{iso} (Voigt)	4.00	6.06	7.91	9.61	10.1	14.0
G^{iso} (Voigt)	1.46	2.26	3.00	3.67	3.87	5.38

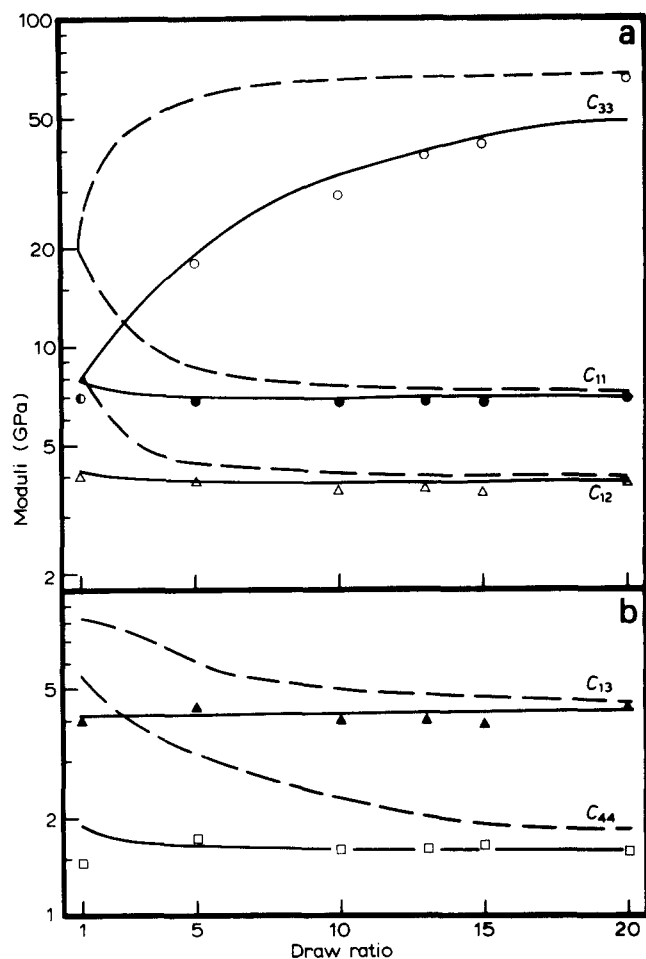


Figure 4 Draw ratio dependence of the elastic moduli of LPE at 0°C obtained from ultrasonic measurements, together with the Voigt (—) and Reuss(---) bounds calculated from the aggregate model assuming pseudo-affine deformation scheme

REFERENCES

- Weeks, N. E. and Porter, R. S. *J. Polym. Sci., Polym. Phys. Edn.* 1974, **12**, 635
- Smith, J. B., Davies, G. R., Capaccio, G. and Ward, I. M. *J. Polym. Sci., Polym. Phys. Edn.* 1975, **13**, 2331
- Gibson, A. G., Davies, G. R. and Ward, I. M. *Polymer* 1978, **19**, 683
- Gibson, A. G., Jawad, S. M., Davies, G. R. and Ward, I. M. *Polymer* 1982, **23**, 349
- Rider, J. G. and Watkinson, K. M. *Polymer* 1978, **19**, 645
- Leung, W. P., Chan, C. C., Chen, F. C. and Choy, C. L. *Polymer* 1980, **21**, 1148
- Gibson, A. G. and Ward, I. M. *J. Polym. Sci., Polym. Phys. Edn.* 1978, **16**, 2015
- Coates, P. D. and Ward, I. M. *Polymer* 1979, **20**, 1439
- Gibson, A. G. and Ward, I. M. *J. Mater. Sci.* 1980, **15**, 979
- Kwan, S. F., Chen, F. C. and Choy, C. L. *Polymer* 1975, **16**, 481
- Jawad, S. M. and Ward, I. M. *J. Mater. Sci.* 1978, **13**, 1381
- Zihlif, A. M., Duckett, R. A. and Ward, I. M. *J. Mater. Sci.* 1978, **13**, 1837
- Zihlif, A. M., Duckett, R. A. and Ward, I. M. *J. Mater. Sci.* 1982, **17**, 1125
- Odajima, A. and Maeda, M. *J. Polym. Sci. C* 1966, **15**, 55
- Tashiro, K., Kobayashi, M. and Tadokoro, H. *Macromolecules* 1978, **11**, 914
- Born, M. and Huang, T. 'Dynamical Theory of Crystal Lattice', Clarendon Press, Oxford, 1956
- Crissman, J. M. and Zapas, L. J. *J. Polym. Sci. A-2* 1977, **15**, 1685
- Boyd, R. H. and Yemni, T. *Polym. Eng. Sci.* 1979, **19**, 1023
- Waterman, H. A. *Kolloid Z.* 1963, **192**, 9
- Ward, I. M. *Proc. Phys. Soc.* 1962, **80**, 1176
- Chan, O. K., Chen, F. C., Choy, C. L. and Ward, I. M. *J. Phys. D: Appl. Phys.* 1978, **11**, 617